

Neutrinoless $\beta\beta$ decay nuclear matrix elements in an isotopic chain

Tomás R. Rodríguez

Institut für Kernphysik, Technische Universität Darmstadt, Schlossgartenstr. 2, D-64289 Darmstadt, Germany

Gabriel Martínez-Pinedo

Institut für Kernphysik, Technische Universität Darmstadt, Schlossgartenstr. 2, D-64289 Darmstadt, Germany

GSI Helmholtzzentrum für Schwerionenforschung, Plankstr. 1, D-64291 Darmstadt, Germany

Abstract

We analyze nuclear matrix elements (NME) of neutrinoless double beta decay calculated for the Cadmium isotopes. Energy density functional methods including beyond mean field effects such as symmetry restoration and shape mixing are used. Strong shell effects are found associated to the underlying nuclear structure of the initial and final nuclei. Furthermore, we show that NME for two-neutrino double beta decay evaluated in the closure approximation, $M_{\text{cl}}^{2\nu}$, display a constant proportionality with respect to the Gamow-Teller part of the neutrinoless NME, $M_{\text{GT}}^{0\nu}$. This opens the possibility of determining the $M_{\text{GT}}^{0\nu}$ matrix elements from β^\mp Gamow-Teller strength functions. Finally, the interconnected role of deformation, pairing, configuration mixing and shell effects in the NMEs is discussed.

1. Introduction

Neutrinoless double beta decay ($0\nu\beta\beta$) is the most promising process to disentangle the Majorana nature of the neutrino, its effective mass and the mass hierarchy [1]. In this process, an even-even nucleus can not energetically decay into the odd-odd neighbor but it is allowed into the even-even nucleus with two protons more and two neutrons less. Only few candidates which fulfill this requirement are found along the nuclear chart in the valley of the stability. Contrary to the two-neutrino double beta decay mode ($2\nu\beta\beta$), where two electrons and two Dirac or Majorana neutrinos are emitted in the final state, the $0\nu\beta\beta$ mode proceeds by exchanging a Majorana neutrino and only two electrons are emitted at a sharp energy equal to the Q -value. $2\nu\beta\beta$ decay has been observed in several isotopes with half-lives 10^{19-21} years. However, except to the controversial claim of the Heidelberg-Moscow experiment [2], the neutrinoless mode has not been measured yet. Nowadays, several experiments devoted to detect this decay mode are presently active or in an advance development phase [3, 4]. If this process is finally detected, the precise determination of the neutrino effective mass depends on the value of the nuclear matrix element (NME). The half-life of this decay, in the so-called light neutrino exchange mechanism, can be written as [1]:

$$\left[T_{1/2}^{0\nu}(0_i^+ \rightarrow 0_f^+)\right]^{-1} = G_{0\nu} |M^{0\nu}|^2 \left(\frac{\langle m_{\beta\beta} \rangle}{m_e}\right)^2 \quad (1)$$

where $G_{0\nu}$ is a well-known kinematic phase space factor [5], $M^{0\nu}$ is the NME, m_e is the electron mass and

$\langle m_{\beta\beta} \rangle$ is the effective Majorana neutrino mass. Several nuclear structure methods have been used so far to calculate these NMEs for the most promising candidates, namely, large scale shell model (SM) [6, 7], quasiparticle random phase approximation (QRPA) [8–10], interacting boson model (IBM) [11], projected Hartree-Fock-Bogoliubov (PHFB) [12] and energy density functional methods (EDF) [13, 14]. In the most recent calculations, the spread in the value of NMEs between different models for a specific candidate is about a factor two. Therefore, it is necessary to study in more detail the NMEs in order to better constraint their values and understand possible relationships between the magnitude of the matrix element and the nuclear structure of parent and daughter states. In this Letter we use energy density functional methods including beyond mean field effects to analyze the NMEs for the decay of Cadmium to Tin isotopes. All of these decays except the one of ^{116}Cd are not physically possible because of the Q -value or because they are strongly hindered by single β^\pm decays. However, these virtual $0\nu\beta\beta$ decays provide useful information about the dependence of the NMEs with the underlying nuclear structure of the mother and daughter nuclei. Therefore, shell effects or the role of deformation and pairing can be studied in a systematic and controllable manner. The paper is organized as follows. The theoretical formalism is described in Sec. 2. Then, the results obtained are reported in Sec. 3. Finally, a summary of the main conclusions is given in Sec. 4.

2. Theoretical framework

We now describe the main aspects of the generator coordinate method (GCM) used to compute the NMEs with energy density functional methods. In this framework, we determine the initial (i) and final (f) states as linear combinations of particle number and angular momentum projected Hartree-Fock-Bogoliubov (HFB) mean-field wave functions [15–19]:

$$|I_{i/f}^{+\sigma}\rangle = \sum_{\beta_2} g_{i/f}^{I\sigma}(\beta_2) |\Psi_{i/f}^I(\beta_2)\rangle \quad (2)$$

where I is the angular momentum, β_2 are intrinsic axial quadrupole deformations, $g_{i/f}^{I\sigma}(\beta_2)$ are the coefficients found by solving the associated Hill-Wheeler-Griffin (HWG) equations [15]:

$$\sum_{\beta_2'} \left(\langle \Psi_{i/f}^I(\beta_2) | \hat{H} | \Psi_{i/f}^I(\beta_2') \rangle - E_{i/f}^{I\sigma} \langle \Psi_{i/f}^I(\beta_2) | \Psi_{i/f}^I(\beta_2') \rangle \right) g_{i/f}^{I\sigma}(\beta_2') = 0 \quad (3)$$

Here, $E_{i/f}^{I\sigma}$ are the energy spectra of the initial/final nuclei and the projected wave functions are defined as:

$$|\Psi_{i/f}^I(\beta_2)\rangle = P^{N_{i/f}} P^{Z_{i/f}} P^I |\phi(\beta_2)\rangle \quad (4)$$

with P^N , P^Z , P^I being the projection operators onto good number of neutrons, protons and angular momentum, respectively. Furthermore, for each deformation β_2 , the HFB-type states $|\phi(\beta_2)\rangle$ are found by minimizing the particle number projected energy with constraints in the mean value of the axial quadrupole moment operator \hat{Q}_{20} , i.e., $\delta(E'^{NZ}(|\phi(\beta_2)\rangle)) = 0$ with [17]:

$$E'^{NZ} = \frac{\langle \phi(\beta_2) | \hat{H} P^N P^Z | \phi(\beta_2) \rangle}{\langle \phi(\beta_2) | \phi(\beta_2) \rangle} - \lambda_{\beta_2} \langle \phi(\beta_2) | \hat{Q}_{20} | \phi(\beta_2) \rangle \quad (5)$$

The Lagrange multiplier λ_{β_2} ensures the condition:

$$\langle \phi(\beta_2) | \hat{Q}_{20} | \phi(\beta_2) \rangle = \frac{\beta_2 3r_0^2 A^{5/3}}{\sqrt{20\pi}} \quad (6)$$

with $r_0 = 1.2$ fm and A the mass number. We use the same interaction both in the determination of the intrinsic states and in the HWG diagonalization, in our case the Gogny D1S force [20]. To solve the HWG equations we transform first Eq. 2 in terms of an orthonormal basis:

$$|\Lambda_{i/f}^I\rangle = \sum_{\beta_2} \frac{u_{\Lambda_{i/f}}^I(\beta_2)}{\sqrt{n_{\Lambda_{i/f}}^I}} |\Psi_{i/f}^I(\beta_2)\rangle; \quad n_{\Lambda_{i/f}}^I > \varepsilon \quad (7)$$

where $u_{\Lambda_{i/f}}^I(\beta_2)$ and $n_{\Lambda_{i/f}}^I$ are the eigenvectors and eigenvalues -greater than a small value $\varepsilon \sim 10^{-5}$ chosen to remove linear dependence of the states- of the norm overlap matrix:

$$\sum_{\beta_2'} \langle \Psi_{i/f}^I(\beta_2) | \Psi_{i/f}^I(\beta_2') \rangle u_{\Lambda_{i/f}}^I(\beta_2) = n_{\Lambda_{i/f}}^I u_{\Lambda_{i/f}}^I(\beta_2) \quad (8)$$

Then, the states given in Eq. 4 can be expressed as $|I_{i/f}^{+\sigma}\rangle = \sum_{\Lambda_{i/f}} G_{\Lambda_{i/f}}^{I\sigma} |\Lambda_{i/f}^I\rangle$ and the HWG equations (Eq. 3) read as:

$$\sum_{\Lambda_{i/f}'} \langle \Lambda_{i/f}^I | \hat{H} | \Lambda_{i/f}'^I \rangle G_{\Lambda_{i/f}'}^{I\sigma} = E_{i/f}^{I\sigma} G_{\Lambda_{i/f}}^{I\sigma} \quad (9)$$

The eigenvectors $G_{\Lambda_{i/f}}^{I\sigma}$ are used to define the relative weight of each deformation β_2 in the GCM wave function, the so-called collective wave functions [15]:

$$F_{i/f}^{I\sigma}(\beta_2) = \sum_{\Lambda_{i/f}} G_{\Lambda_{i/f}}^{I\sigma} u_{\Lambda_{i/f}}^I(\beta_2) \quad (10)$$

In addition, any expectation value between GCM wave functions (energies, radii, transitions, etc.) can be expressed in terms of these coefficients, as we will see in the case of $0\nu\beta\beta$ NMEs.

It is important to underline that, in this framework, particle number and rotational symmetries are conserved by projecting the intrinsic HFB wave functions and, in addition, shape mixing is naturally included and self-consistently determined by solving the HWG equations. On the other hand, the main restrictions of the model come from the symmetries imposed to the HFB-type states $|\phi(\beta_2)\rangle$. They are tensorial products of proton and neutron wave functions (no isospin mixing), and are also parity and axially symmetric. Work is in progress to check the effect of these approximations in the NMEs. Finally, a large configuration space including eleven major harmonic oscillator shells and sets of 56 states with different deformation ranging from $\beta_2 \in [-0.5, 0.6]$ are used in this work.

Once the initial and final states are found, we proceed to evaluate the NMEs as the sum of Fermi (F) and Gamow-Teller (GT) terms [1] (tensor contribution is neglected in this work [7, 10]):

$$M^{0\nu} = - \left(\frac{g_V}{g_A} \right)^2 M_F^{0\nu} + M_{GT}^{0\nu} \quad (11)$$

with $g_V = 1$ and $g_A = 1.25$ being the vector and axial coupling constants. First, we use the closure approximation to by-pass the calculation of the odd-odd intermediate nucleus. This approximation is expected to be a good one in the $0\nu\beta\beta$ case [1, 21]. Then, the NMEs can be determined as the expectation value of two-body operators between the initial and final states:

$$M_{F/GT}^{0\nu} = \langle 0_f^+ | \hat{M}_{F/GT}^{0\nu} | 0_i^+ \rangle \quad (12)$$

with:

$$\hat{M}_F^{0\nu} = \left(\frac{g_A}{g_V} \right)^2 \sum_{i < j} \hat{V}_F(r_{ij}) \hat{\tau}_-^{(i)} \hat{\tau}_-^{(j)}, \quad (13)$$

$$\hat{M}_{GT}^{0\nu} = \sum_{i < j} \hat{V}_{GT}(r_{ij}) (\hat{\sigma}^{(i)} \cdot \hat{\sigma}^{(j)}) \hat{\tau}_-^{(i)} \hat{\tau}_-^{(j)} \quad (14)$$

In these expressions, $\hat{\tau}_-$ is the isospin ladder operator that changes neutrons into protons and $\hat{\sigma}$ are the Pauli matrices acting on the spin part of the wave functions. The

so-called neutrino potentials $\hat{V}_{F/GT}$ depend on the relative distance between two nucleons. These potentials take into account nucleon finite size corrections and higher order currents [8] (see Refs. [7, 8] for detailed expressions). Before including short-range correlations within the UCOM framework [9, 22] the neutrino potentials can be expressed as an integral in the momentum transferred q of the Fermi or Gamow-Teller form factor $h_{F/GT}(q)$ weighted by the spherical Bessel function $j_0(qr)$ [7, 8]:

$$V_{F/GT}(r) = \frac{2}{\pi} \frac{r_0 A^{1/3}}{g_A^2} \int_0^\infty j_0(qr) \frac{h_{F/GT}(q)}{q + \mu} q dq \quad (15)$$

For the sake of simplicity we take the same value of the closure energy $\mu = 10.22$ MeV for the whole isotopic chain. This value is the one used for computing the NME of ^{116}Cd decay in Ref. [13].

We now calculate the NMEs (Eq. 12) with the EDF formalism described above. We take the ground states given by the lowest energy solution of the HWG equation with ($I = 0, \sigma = 1$) and evaluate:

$$M_{F/GT}^{0\nu} = \sum_{\substack{\Lambda_f \Lambda_i \\ \beta_2 \beta'_2}} G_{\Lambda_f}^{*0,1} \frac{u_{\Lambda_f}^{*0}(\beta_2)}{\sqrt{n_{\Lambda_f}^0}} \frac{u_{\Lambda_i}^0(\beta_2)}{\sqrt{n_{\Lambda_i}^0}} G_{\Lambda_i}^{0,1} \bar{M}_{F/GT}^{0\nu}(\beta_2, \beta'_2) \quad (16)$$

where $\bar{M}_{F/GT}^{0\nu}(\beta_2, \beta'_2) = \langle \Psi_f^0(\beta_2) | \hat{M}_{F/GT}^{0\nu} | \Psi_i^0(\beta'_2) \rangle$. The last expression, properly normalized, gives the explicit dependence of the NMEs with the quadrupole deformation of the mother and daughter nuclei:

$$M_{F/GT}^{0\nu}(\beta_2, \beta'_2) = \frac{\bar{M}_{F/GT}^{0\nu}(\beta_2, \beta'_2)}{\sqrt{\langle \Psi_f^0(\beta_2) | \Psi_f^0(\beta_2) \rangle \langle \Psi_i^0(\beta'_2) | \Psi_i^0(\beta'_2) \rangle}} \quad (17)$$

The final value of the NME can be approximately interpreted as the convolution of the collective wave functions of initial and final states (Eq. 10) with the intensity of the Fermi and GT NMEs as a function of the deformation given in Eq. 17.

3. Results

We now show the results of the $0\nu\beta\beta$ NMEs in the cadmium isotopic chain $^{98-132}\text{Cd}$. This set of nuclei covers the shells from $N = 50$ to $N = 82$ magic numbers both in the mother (Cd) and daughter (Sn) isotopes. We first describe the ground states of these nuclei that are the ones involved in the $0\nu\beta\beta$ decay. In Fig. 1 the experimental [23] and theoretical $Q_{\beta-\beta--}$ values are plotted. We observe that experimental and theoretical data almost run parallel each other, increasing the value continuously with increasing the mass number from negative to positive values. Additionally, a quantitative agreement is found within the limit of accuracy of the Gogny D1S force, which is approximately 3.4 MeV [24]. Nevertheless, the theoretical result

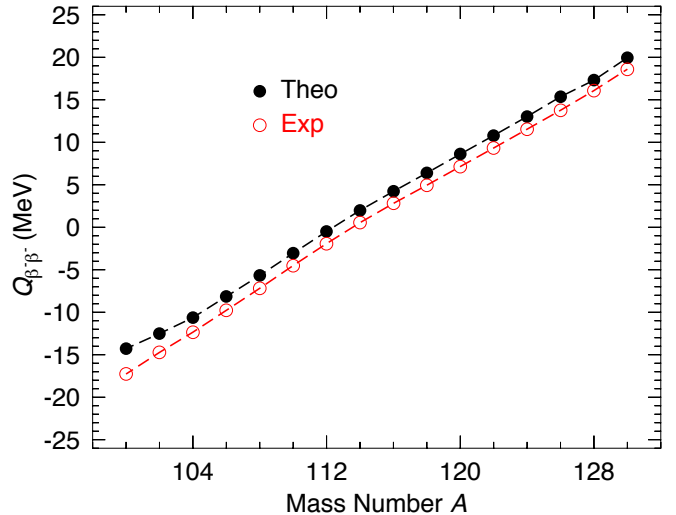


Figure 1: (color online) Experimental [23] and theoretical $Q_{\beta-\beta--}$ value for cadmium isotopes as a function of the mass number A .

overestimates the $Q_{\beta-\beta--}$ value about ~ 1.4 MeV. It is important to point out that no tuning of the parameters of the interaction has been made.

In Fig. 2 we represent the evolution from shell to shell of the ground state collective wave functions (Eq. 10) for Cd -Fig. 2(a)- and Sn -Fig. 2(b)- isotopes. First of all, we observe that the distributions are enclosed around $\beta_2 \sim [-0.2, 0.2]$ for all nuclei, i.e., these are not very deformed systems. In addition, most of the collective wave functions present two maxima, one oblate and one prolate, with a minimum in the spherical point. This is not the case for the magic or their nearest neighbor nuclei ($^{98,130-132}\text{Cd}$ and $^{98-102,130-132}\text{Sn}$) whose collective wave functions also peak in the spherical point. For the Cd chain (Fig. 2(a)) prolate maxima are higher than the oblate ones while a more symmetric distribution around $\beta_2 = 0$ is obtained for the Sn isotopes. In addition, mirror nuclei ^{98}Cd and ^{98}Sn have almost identical collective wave functions as one could expect.

A more quantitative analysis of the deformation can be done by representing in Fig. 3(a) the mean value $\bar{\beta}_2$ for the collective wave functions given above. We see in Fig. 3(a) that tin isotopes are spherical or very little oblate deformed in the mid-shell ($\bar{\beta}_2 \sim -0.025$ for ^{114}Sn) as it is expected from its proton shell closure $Z = 50$. On the other hand, the mean deformation in cadmium isotopes is zero only in the shell closures $N = 50, 82$ while the rest of nuclei are slightly prolate deformed. Hence, we find two maxima at $^{104,106}\text{Cd}$ and ^{118}Cd with $\bar{\beta}_2 \sim 0.12$ and $\bar{\beta}_2 \sim 0.10$ respectively and a local minimum at ^{112}Cd ($\bar{\beta}_2 \sim 0.08$).

The effect of the deformation of initial and final states and the role played by pairing correlations on the NMEs for individual decays have been already discussed extensively within the EDF framework [13, 14], and, to a lesser

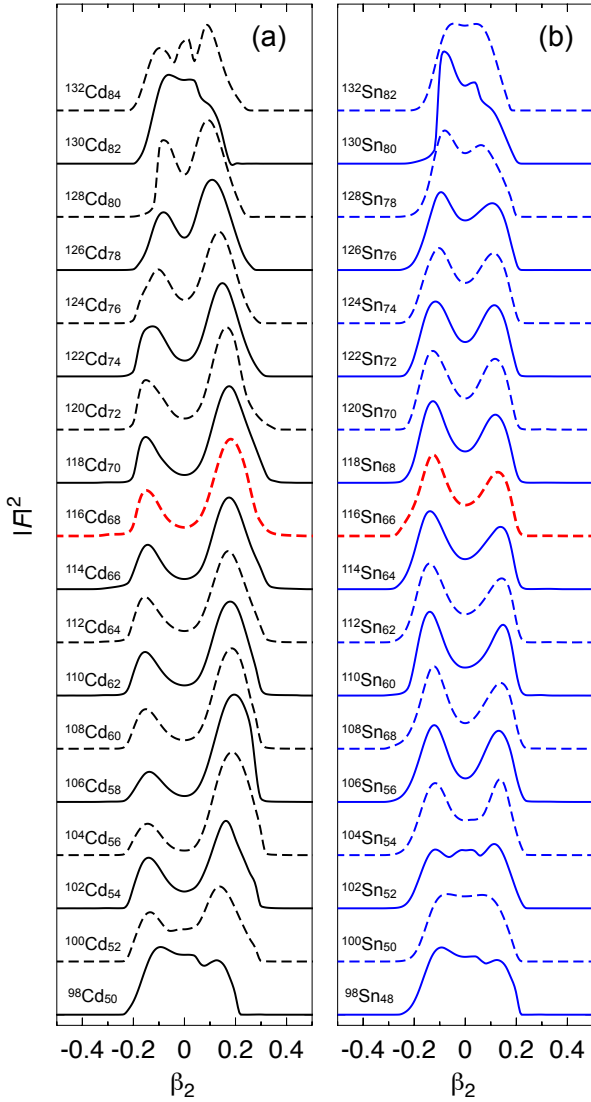


Figure 2: (color online) Ground state 0^+ collective wave functions for (a) cadmium and (b) tin isotopes calculated with the Gogny D1S EDF. ^{116}Cd (^{116}Sn) double beta emitter is represented in red.

extent, within the shell model [25], QRPA [26] and IBM [11] approaches. On the one hand, a strong suppression of the NMEs is found for decays between states with different intrinsic deformations. Furthermore, shape mixing effects tend to reduce the values of the matrix elements calculated assuming only spherical symmetry [14, 27]. On the other hand, the NMEs are enhanced if a large amount of pairing correlations are present, or in the shell model language, when the wave functions are dominated by general-ize seniority zero components, in the mother and daughter nuclei [6, 13]. Let us study now if these conclusions can be extended to the NMEs calculated in the Cd isotopic chain where the number of neutrons changes smoothly within a major shell.

In Fig. 3(b) we compare the values of the NMEs obtained from the full configuration mixing (Eq. 16) with

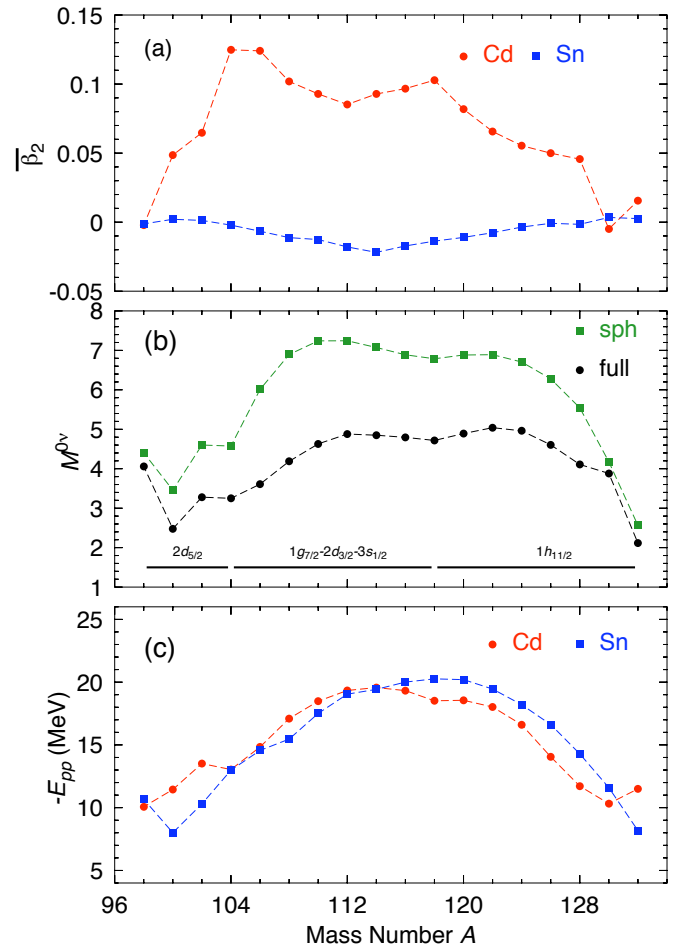


Figure 3: (color online) (a) Mean value of the quadrupole deformation β_2 for the collective wave functions given in Fig. 2. (b) Nuclear matrix elements for initial and final nuclei considered as spherical systems (filled squares) and including the full shape mixing (filled circles). (c) Total pairing energies for Cd and Sn isotopes including shape configuration mixing.

those assuming spherical shapes $M^{0\nu}(\beta_2 = 0, \beta'_2 = 0)$ (Eq. 17) for mother and daughter nuclei. We observe that, except for the transition between mirror nuclei $A = 98$, $M^{0\nu}$ is small near the neutron shell closures. Furthermore, the NMEs for the spherical shape are always larger than the ones which include configuration mixing although both curves show a similar structure. The reduction obtained by shape mixing is smaller near the shell closures where the relevant deformations explored by the collective wave functions are precisely the spherical ones. From Fig 3(a) we can also see qualitatively that the larger is the difference between the mean quadrupole deformation of mother and daughter nuclei the larger is the reduction of the NME with respect to its spherical value. This shows that the correlation observed between the value of NME and differences in nuclear deformation is a general feature of neutrinoless double beta-decay and not a particular aspect of those beta-decays studied so far [13].

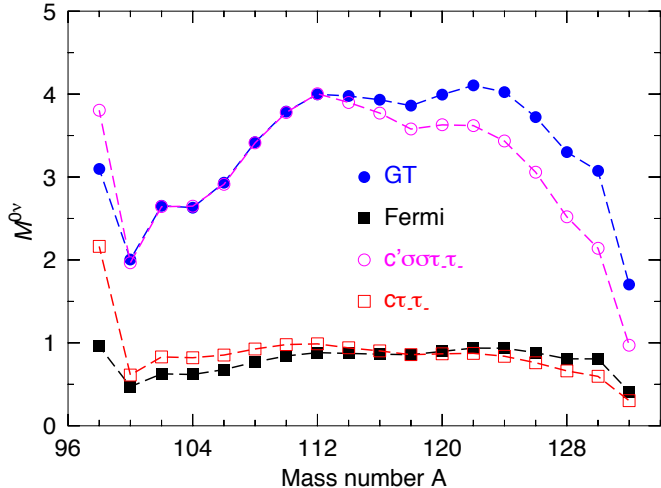


Figure 4: (color online) Nuclear matrix elements calculated with Fermi (squares), Gamow-Teller (bullets) and constant neutrino potentials $V_F(r) = c = 2.0$ (boxes) and $V_{GT}(r) = c' = 2.0$ (circles)

We now analyze the structure of the NMEs along the isotopic chain (Fig. 3(b)). First, we observe a large value of the NME for $A = 98$ transition between mirror nuclei. The wave functions of the initial and final states are practically identical (see Fig. 2) and their overlap is therefore maximized [25]. Apart from this specific case, the rest of the curve shows some structure that can be related to neutron sub-shell closures in Cd isotopes. In Ref. [11] shell effects are studied within a generalized seniority scheme and it is observed that the lowest NME values correspond to the shell closures and a maximum is found at the mid-shell. The same behavior can be also seen in Fig. 3(b) where three maxima are found at $A(N) = 102(54)$, $112(64)$ and $122(74)$ that can be related to the half-filling of $2d_{5/2}$, $1g_{7/2}3s_{1/2}2d_{3/2}$ and $1h_{11/2}$ sub-shells. The local minimum found at $A = 118$ would correspond to the crossing of the $1g_{7/2}3s_{1/2}2d_{3/2}$ sub-shell.

These shell effects are also related to the content of pairing correlations in initial and final nuclei as we can see in Fig 3(c). In this figure we represent the pairing energy ($-E_{pp}$) [15] evaluated with the GCM states given in Eq. 2. In closed shell nuclei, $N = 50$ and $N = 82$, pairing correlations are significantly smaller than in open-shell nuclei, obtaining the parabolic shape given in the figure. Nevertheless, we also find local minima in the Cd isotopic chain at $A = 104$ and $A = 118$ related to the sub-shell closures described above. Therefore, we obtain again a direct generalization of a result already found in individual decays, namely, the utter connection between pairing correlations in the initial and final nuclei and the NMEs.

Finally we study the sensitivity of the NMEs to the form of the neutrino potentials $V_{F/GT}(r)$ given in Eq. 15. In Fig. 4 we compare the Fermi and GT components of $M^{0\nu}$ assuming a constant neutrino potential, i.e. indepen-

dent of the relative distance of the decaying neutrons, with those obtained using the usual form (15). We take as 2.0 the constant value of the neutrino potential as it reproduces both the Fermi and Gamow-Teller NME computed using the full potential. The same pattern is found for the NMEs calculated with a constant spatial dependence and the ones given by the full neutrino potentials, i.e., similar enhancement of $M^{0\nu}$ in mirror nuclei and shell effects both for Fermi and Gamow-Teller parts. This shows that the overall behavior of the NME is quite insensitive to the details of the neutrino potential. Nevertheless, the NMEs computed with regular neutrino potentials are more symmetric with respect to the local minimum found at $A = 118$, while the ones computed with constant potentials are smaller after this minimum. This fact is related to the filling of the negative parity $1h_{11/2}$ sub-shell and could be associated to a increased contribution of multipoles of higher order than the Gamow-Teller, i.e. the only one present in the constant potential case.

This proportionality is important because the GT part calculated with a constant potential is directly related to the $2\nu\beta\beta$ matrix element evaluated in the closure approximation [21]:

$$M_{cl}^{2\nu} = \langle 0_f^+ | \sum_{i < j} \hat{\sigma}^{(i)} \cdot \hat{\sigma}^{(j)} \hat{\tau}_-^{(i)} \hat{\tau}_-^{(j)} | 0_i^+ \rangle \quad (18)$$

Limits on this matrix element can be experimentally obtained from charge exchange reactions (see [28] and references therein) or assuming single-state dominance hypothesis [29]. Hence, it would help to constrain experimentally the value of $M_{GT}^{0\nu}$. In this work we obtain for ^{116}Cd an unquenched value of $M_{cl}^{2\nu} = 1.885$ which is much larger than the one extracted from charge exchange reactions [28] $M_{cl,cer}^{2\nu} = 0.314$. However, the GT operator would require a quenching factor to account for renormalization effects of the weak-axial current. On the other hand, the experimental data reported on [28] includes GT strength located at excitation energies below 3 MeV in the intermedium nucleus. One expects substantial contributions to the $M_{cl}^{2\nu}$ from states in the GT resonance at excitation energies around 10 MeV. Notice, that these transitions are suppressed for the regular $M^{2\nu}$ matrix element [21] due to the energy denominator but not for the $M_{cl}^{2\nu}$ matrix element. Based on QRPA calculations ref. [21] shows that a converged value of $M_{cl}^{2\nu}$ requires the inclusion of states up to 15 MeV excitation energy in the intermedia nucleus. Further work is in progress to determine the origin of this proportionality which has also been observed, within the EDF framework, in the NMEs as a function of deformation of individual decays [14], and in shell model calculations [25], but not found in QRPA calculations [21].

4. Summary

In summary, we have studied the $0\nu\beta\beta$ nuclear matrix elements in the cadmium isotopic chain with energy

density functional methods. It is shown that previous correlations found for individual decays between the magnitude of the NME and pairing correlations, deformation, shell effects and shape of the neutrino potential can be extended to a whole isotopic chain. This shows that this correlations are a particular feature of the NME that is independent of the detailed structure of the nuclear wave functions. Large NMEs are obtained if the pairing correlations in the initial and final states are considerable and the difference in deformation is small. Furthermore, the NMEs are very sensitive to the sub-shell closures. In addition, the NME for mirror nuclei is enhanced due to the large overlap between mother and daughter wave functions. Finally, NMEs calculated neglecting the neutrino potential, i.e. the two-neutrino double beta-decay matrix element evaluated in the closure approximation, are found to exhibit a nearly constant proportionality to the realistic ones. This opens the possibility of constraining the $M^{0\nu}$ matrix element from the knowledge of the β^\mp Gamow-Teller strength functions.

We thank J. Menéndez and A. Poves for stimulating discussions. This work was partly supported by the Helmholtz International Center for FAIR within the framework of the LOEWE program launched by the State of Hesse, by the Deutsche Forschungsgemeinschaft through contract SFB 634 and by the BMBF-Verbundforschungsprojekt number 06DA7047I.

References

- [1] F. T. Avignone, S. R. Elliot, J. Engel, *Rev. Mod. Phys.* **80**, 481 (2008).
- [2] H. V. Klapdor-Kleingrothaus *et al.*, *Phys. Lett. B* **586**, 198 (2004).
- [3] H. Ejiri, *Prog. Part. Nucl. Phys.* **64**, 249 (2010).
- [4] A. S. Barabash, *Phys. At. Nucl.* **74**, 603 (2011).
- [5] J. Kotila and F. Iachello, *Phys. Rev. C* **85**, 034316 (2012).
- [6] E. Caurier *et al.*, *Phys. Rev. Lett.* **100**, 052503 (2008).
- [7] J. Menéndez *et al.*, *Nucl. Phys. A* **818**, 139 (2009).
- [8] F. Šimkovic *et al.*, *Phys. Rev. C* **60**, 055502 (1999).
- [9] F. Šimkovic *et al.*, *Phys. Rev. C* **77**, 045503 (2008).
- [10] M. Kortelainen, J. Suhonen, *Phys. Rev. C* **75**, 051303(R) (2007).
- [11] J. Barea and F. Iachello, *Phys. Rev. C* **79**, 044301 (2009).
- [12] K. Chaturvedi *et al.*, *Phys. Rev. C* **78**, 054302 (2008).
- [13] T. R. Rodríguez and G. Martínez-Pinedo, *Phys. Rev. Lett.* **105**, 252503 (2010).
- [14] T. R. Rodríguez and G. Martínez-Pinedo, *Prog. Part. Nucl. Phys.* **66**, 436 (2011).
- [15] P. Ring, P. Schuck, *The nuclear many body problem*, Springer-Verlag, Berlin, 1980.
- [16] M. Bender, P.-H. Heenen, P.-G. Reinhard, *Rev. Mod. Phys.* **75**, 121 (2003).
- [17] M. Anguiano, J. L. Egido, L. M. Robledo, *Nucl. Phys. A* **696**, 467 (2001).
- [18] R. R. Rodríguez-Guzmán, J. L. Egido, L. M. Robledo, *Nucl. Phys. A* **709**, 201 (2002).
- [19] T.R. Rodríguez, J.L. Egido, *Phys. Rev. Lett.* **99**, 062501 (2007).
- [20] J. F. Berger *et al.*, *Nucl. Phys. A* **428**, 23 (1984).
- [21] F. Šimkovic, R. Hodák, A. Faessler, and P. Vogel, *Phys. Rev. C* **83**, 015502 (2011).
- [22] H. Feldmeier, T. Neff, R. Roth, J. Schnack, *Nucl. Phys. A* **632**, 61 (1998).
- [23] G. Audi, A.H. Wapstra, C. Thibault, *Nucl. Phys. A* **729**, 337 (2003).
- [24] S. Hilaire and M. Girod, *Eur. Phys. J. A* **33**, 237 (2007).
- [25] J. Menéndez *et al.* *J. Phys.: Conf. Ser.* **267**, 012058 (2011).
- [26] D. -L. Fang, A. Faessler, V. Rodin, and F. Šimkovic, *Phys. Rev. C* **83**, 034320 (2011).
- [27] T.R. Rodríguez and Gabriel Martínez-Pinedo, *Phys. Rev. C* **85**, 044310 (2012).
- [28] S. Rakers *et al.*, *Phys. Rev. C* **71**, 054313 (2005).
- [29] J. Abad, A. Morales, R. Núñez Lagos and A.F. Pacheco, *An. Fis. A80*, 9 (1984).